

Contents lists available at [SciVerse ScienceDirect](http://www.sciencedirect.com)

Spectrochimica Acta Part A: Molecular and Biomolecular Spectroscopy

journal homepage: www.elsevier.com/locate/saaA new 1,8-naphthalimide-based colorimetric and “turn-on” fluorescent Hg^{2+} sensorZhiyuan Zhang^a, Yuhua Chen^b, Dongmei Xu^{a,*}, Liang Yang^a, Aifeng Liu^a^a College of Chemistry, Chemical Engineering and Materials Science, National Engineering Laboratory for Modern Silk, Key Laboratory of Organic Synthesis of Jiangsu Province, Jiangsu Key Laboratory of Advanced Functional Polymer Design and Application, Soochow University, Suzhou, Jiangsu 215123, China^b College of Pre-clinical Medical and Biological Science, Soochow University, Suzhou 215123, China

HIGHLIGHTS

- ▶ A new molecule for optically sensing Hg^{2+} in aqueous solutions is reported.
- ▶ Its UV–vis absorption and fluorescence spectra were carefully studied.
- ▶ The spectra are almost insensitive to H^+ within a wide range of pH.
- ▶ The spectra are highly selective and sensitive to Hg^{2+} .
- ▶ The spectra changes are the coefficient results of PET and ICT.

GRAPHICAL ABSTRACT



ARTICLE INFO

Article history:

Received 19 August 2012

Received in revised form 20 November 2012

Accepted 30 November 2012

Available online 20 December 2012

Keywords:

1,8-Naphthalimide

Colorimetric

Fluorescent sensor

Fluorescence sensor

 Hg^{2+}

ABSTRACT

A new fluorescent molecule 4-(bis(2-(ethylthio)ethyl)amino)-N-n-butyl-1,8-naphthalimide (BTABN) was reported. Its UV–vis absorption and fluorescence spectra were almost not dependent on the pH, but remarkably and selectively affected by Hg^{2+} . Upon the addition of Hg^{2+} in EtOH/ H_2O (1/2, v/v), the absorption wavelength maxima were blueshifted from 436 nm to 376 nm with a naked-eye observed color change, and the fluorescence was greatly enhanced with a 14 nm blueshift within 1 min. Na^+ , K^+ , Ca^{2+} , Mg^{2+} , Cu^{2+} , Zn^{2+} , Cr^{3+} , Pb^{2+} , Ni^{2+} , Fe^{2+} , Mn^{2+} , Co^{2+} , Cd^{2+} showed no obvious interferences with the detection. The binding stoichiometry indicates that a 1:1 complex is formed between Hg^{2+} and BTABN. The response of the UV–vis absorption and the fluorescence spectra to Hg^{2+} can be attributed to the joint contribution of the PET and ICT process.

© 2012 Elsevier B.V. All rights reserved.

Introduction

Mercury and its compounds are widely used in appliances and instruments, metallurgy, chemical industry, medicine, and military, and easily enter the environment, including air, soil and water. Hg^{2+} can be bioaccumulated in the brain and kidney through food chain and atmospheric circulation and seriously threaten people's health by resulting in the central nervous and

reproductive development system damage [1,2]. As one of the most toxic heavy metal ions, its detection is of great importance. Among plenty of methods for detecting Hg^{2+} , fluorescent sensor becomes the most valuable one because of its high selectivity and sensitivity, easy operation, fast response, low cost and real time monitoring [3,4]. A large number of articles regarding fluorescence detection of Hg^{2+} have been published [5,6]. Most of the sensors are based on fluorescein [7], benzoxadiazole [8], coumarin [9], rhodamine [10–15], cyanine [16–18] and 1,8-naphthalimide [19–21]. However, many of these sensors have shortcomings such as cross-sensitivity toward other metal ions, short emission wavelengths, sensitivity to pH and low water solubility. Therefore, the design of better sensors for rapid detection of Hg^{2+} in the environment and biological systems is very meaningful.

* Corresponding author. Address: College of Chemistry, Chemical Engineering and Materials Science, Soochow University, No. 199 Ren-ai Road, Suzhou Industrial Park, Suzhou, Jiangsu 215123, China. Tel.: +86 512 65882027; fax: +86 512 65880089.

E-mail address: xdm.sd@163.com (D. Xu).

1,8-Naphthalimide is a favorite reporter for fluorescent sensors owing to its high absorption coefficient, high fluorescence and quantum yield, large Stokes shift, good photostability and easy to modification. N, S and O, especially S atom, are commonly used potential binding sites for Hg^{2+} [5,6]. Therefore, in this work, we designed and synthesized a novel fluorescent sensor for Hg^{2+} by attaching a functional group containing one N and two S atoms to the C-4 position of 1,8-naphthalimide. The effects of proton and metal ions on the UV–vis absorption and fluorescence spectra of the sensor were carefully studied, and the binding mode and the sensing mechanism were investigated.

Experimental

Materials, instruments and methods

Materials

4-Bromo-1,8-naphthalic anhydride (BNA) (98%) were supplied by Anshan HIFI Chemical Co., Ltd. n-Butylamine (n-BA), diethanolamine (DEA), SOCl_2 of analytical grade were bought from Sinopharm Chemical Reagent Co., Ltd. NaH (55–65% in kerosene), bis(2-chloroethyl)amine hydrochloride and ethanethiol (EtSH) (99%) were purchased from J&K Chemical Co., Ltd. NaCl, KCl, MgCl_2 , CaCl_2 , $\text{CrCl}_3 \cdot 6\text{H}_2\text{O}$, $\text{MnSO}_4 \cdot \text{H}_2\text{O}$, $\text{FeCl}_3 \cdot 6\text{H}_2\text{O}$, $\text{FeCl}_2 \cdot 7\text{H}_2\text{O}$, $\text{CoCl}_2 \cdot 6\text{H}_2\text{O}$, $\text{Ni}(\text{NO}_3)_2 \cdot 6\text{H}_2\text{O}$, $\text{CuCl}_2 \cdot 2\text{H}_2\text{O}$, $\text{Zn}(\text{NO}_3)_2 \cdot 6\text{H}_2\text{O}$, $\text{CdCl}_2 \cdot 2.5\text{H}_2\text{O}$, HgCl_2 and $\text{Pb}(\text{NO}_3)_2$ were the metal cations sources, which were provided by Sinopharm Chemical Reagent Co., Ltd. All the reagents were used as received. The solvents used in synthesis were of analytical grade, others were spectroscopy grade. They were used without special treatment.

Instruments

IR was recorded on a Nicolet Magan-550 spectrometer (Nicolet Co., USA). LC–MS was collected on an Agilent 1200/6220 spectrometer (Agilent Co., USA). ^1H NMR and ^{13}C NMR spectra were carried out on a 400 and 100 MHz Varian Unity Inova spectrometer (Varian Co., USA) respectively. The elementary analysis was measured on a Carlo-Erba EA1110 CHNO-S (Carlo-Erba Co., Italy). UV–vis spectra were obtained on a U-3900 spectrophotometer (Perkin–Elmer Co., USA). Fluorescence spectra were taken on a Fluoromax-4 spectrofluorometer (Slit width: 5 nm). pH values were measured on a Mettler-Toledo FE20 pH meter (Mettler-Toledo Co., USA). Melting point was determined on an X-6 Microscopic melting point tester (Beijing Tech Instrument Co., Ltd., China). All the pH values and the spectral measurements were performed at 25 °C.

Methods

BTABN was dissolved in dichloromethane to form 2 mM stock solutions. Metal salts were dissolved in deionized water to get

10 mM stock solutions. When examining the fluorescence response of BTABN upon pH, 50 μL stock solution of BTABN was taken into 10 mL volumetric flasks, volatilized CH_2Cl_2 and diluted to 10 μM with ethanol (EtOH) and Britton–Robinson buffer at different pH in a volume ratio of 1/2 (1/2, v/v). When studying the fluorescence sensing behaviors of BTABN to metal ions, 50 μL stock solution of BTABN was put into a 10 mL volumetric flask, volatilized CH_2Cl_2 , mixed with 100 μL one of the stock solutions of the metal salts, and diluted with EtOH/ H_2O (1/2, v/v) in sequence. The concentration of BTABN and metal ions was 10 μM and 100 μM , respectively. In the UV–vis absorption and fluorescence titration, the mixed stock solutions of Hg^{2+} salt varied from 0 to 500 μL and the concentration of Hg^{2+} was 0–500 μM .

When the fluorescent quantum yield (Φ_s) of BTABN was evaluated, the absorbance of the solutions was controlled less than 0.05 in order to make the testing results reliable. Φ_s was estimated from the absorption and fluorescence spectra of BTABN according to Eq. (1), where the subscript s and r stand for the sample and reference (rhodamine B, $\Phi_r = 0.97$ in ethanol), respectively. Φ is the quantum yields, A represents the absorbance at the excitation wavelength, S refers to the integrated emission band areas and n_D is the solvent refractive index.

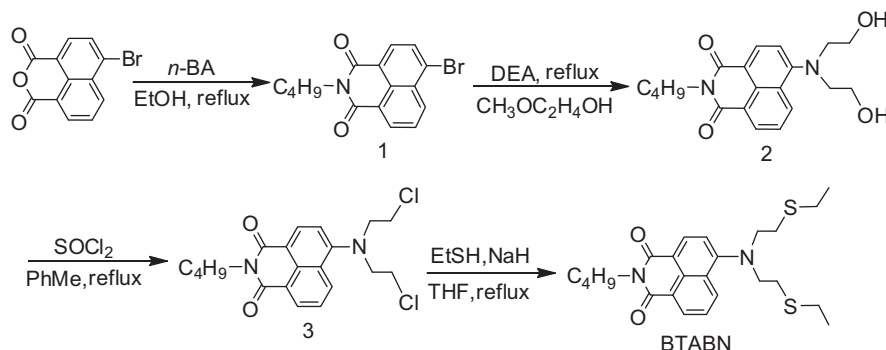
$$\Phi_s = \Phi_r \frac{S_s A_r n_{Ds}^2}{S_r A_s n_{Dr}^2} \quad (1)$$

Synthetic procedures and characterization data

BTABN was synthesized from 4-bromo-1,8-naphthalic anhydride (BNA), n-butylamine (n-BA), diethanolamine (DEA), SOCl_2 and ethanethiol (EtSH) by four steps, as shown in Scheme 1.

Intermediate

Intermediate 1 was synthesized by the reaction between BNA and n-BA, according to Ref. [22]. Its melting point was 104–105 °C, as reported in the reference. Intermediate 1 reacted with DEA to afford intermediate 2, as described in Ref. [23]. ^1H NMR (CDCl_3 , 400 MHz) δ (ppm): 0.95 (3H, t, $J = 8.0$ Hz), 1.41 (2H, m), 1.66 (2H, m), 3.60 (4H, t, $J = 5.0$ Hz), 3.86 (4H, t, $J = 5.0$ Hz), 4.08 (2H, t, $J = 8.0$ Hz), 7.33 (1H, d, $J = 8.0$ Hz), 7.58 (1H, t, $J = 8.0$ Hz), 8.38 (1H, d, $J = 8.0$ Hz), 8.41 (1H, d, $J = 8.0$ Hz), 8.84 (1H, d, $J = 8.0$ Hz). LC–MS $[\text{M}+\text{H}]^+$: m/z , found. 357.1812. Calcd. 357.1800. The characterization data were in accordance with that reported in the reference. Intermediate 2 (0.4 g, 1.12 mM) was dissolved in toluene (PhMe) (10 mL) and added SOCl_2 (2 mL, 27.5 mM). After reflux for 7 h, the solvent was evaporated under reduced pressure, and the residue was purified by column chromatography using CH_2Cl_2 as eluent to afford intermediate 3 (0.35 g, yield: 81.5%). IR (KBr pellet, cm^{-1}): 2960, 2929, 2869, 1694, 1656, 1592, 1466,



Scheme 1. Synthetic route of BTABN.

1396, 1356, 785, 759. ^1H NMR (CDCl_3 , 400 MHz) δ (ppm): 0.98 (3H, t, $J = 7.5$ Hz), 1.45 (2H, m), 1.73 (2H, m), 3.59 (4H, t, $J = 6.5$ Hz), 3.80 (4H, t, $J = 6.5$ Hz), 4.18 (2H, t, $J = 7.5$ Hz), 7.46 (1H, d, $J = 8.0$ Hz), 7.75 (1H, t, $J = 7.5$ Hz), 8.55 (2H, t, $J = 8.5$ Hz), 8.61 (1H, d, $J = 7.5$ Hz). LC–MS $[\text{M}+\text{H}]^+$: m/z , found. 393.1130. Calcd. 393.1100.

BTABN

To a solution of NaH (0.15 g, 6.25 mM) and EtSH (3 mL, 40.4 mM) in dry tetrahydrofuran (THF) (15 mL), intermediate 3 (0.2 g, 0.5 mM) in dry THF (5 mL) was added dropwise over 10 min under stirring. The mixture was refluxed for 48 h, then the solvent was evaporated under reduced pressure and the residue was purified by column chromatography using ethyl acetate/cyclohexane (1/10, v/v) as eluent to afford BTABN (0.12 g, yield: 54.1%). IR (KBr pellet, cm^{-1}): 2959, 2928, 2869, 1695, 1655, 1591, 1465, 1397, 1356, 784, 760. ^1H NMR (CDCl_3 , 300 MHz) δ (ppm): 0.902 (3H, t, $J = 7.2$ Hz), 1.215 (6H, t, $J = 7.5$ Hz), 1.448 (2H, m), 1.703 (2H, m), 2.474 (4H, m), 2.703 (4H, t, $J = 7.5$ Hz), 3.611 (4H, t, $J = 7.2$ Hz), 4.177 (2H, t, $J = 7.5$ Hz), 7.327 (1H, d, $J = 8.1$ Hz), 7.691 (1H, t, $J = 8.1$ Hz), 8.494 (2H, d, $J = 7.8$ Hz), 8.575 (1H, d, $J = 7.2$ Hz). ^{13}C NMR (CDCl_3 , 100 MHz) δ (ppm): 13.90, 20.08, 30.03, 31.36, 32.15, 38.09, 39.97, 41.00, 53.61, 55.25, 117.76, 118.55, 123.10, 126.07, 127.70, 129.83, 130.07, 131.46, 152.38, 163.90. LC–MS $[\text{M}+\text{H}]^+$: m/z , found. 445.1980. Calcd. 445.1900. Elementary analysis: $\text{C}_{24}\text{H}_{32}\text{N}_2\text{O}_2\text{S}_2$ (444.1900); Calcd. (%): C 64.14, H 7.29, N 6.21, found (%): C 64.83, H 7.25, N 6.30.

Results and discussion

Design and synthesis of BTABN

The photoinduced electron transfer (PET) system is one of the most popular approaches to the design of “turn-on” fluorescent sensors. However, the PET-based sensors are usually pH sensitive, which interferes in the detection of other cations. Intramolecular charge transfer (ICT) is another important mechanism for the design of optical sensors. ICT-based sensors have obvious blueshift or redshift in the UV–vis absorption and fluorescence spectra, accompanied by naked eye color changes. However, they generally do not exhibit remarkable fluorescence enhancement. It can be rationally imagined that highly selective and sensitive colorimetric and “turn-on” optical sensors can be achieved if the advantages of the PET and ICT-based sensors are integrated. 1,8-Naphthalimide is one of the most suitable fluorophores for building PET and ICT-based sensors [19–21,24–26]. The functional groups containing N, S and O, especially S atom, are frequently-used ligand for Hg^{2+} [5,6]. Therefore, a thioether-rich bis[2-(ethylthio)ethyl]amino group is chosen as the receptor and attached to the C-4 position of the 1,8-naphthalimide. The binding ability of the S atom to proton is weaker than that of the N atom, leading to the possibility of eliminating the PET-caused pH sensitivity, while the thiophilic nature of mercury can arouse PET-caused fluorescence enhancement. The extreme affinity of Hg^{2+} to sulfur over other metal ions can improve the specificity of the sensor [27]. In addition, the N atom directly linked to the C-4 position of the naphthalene ring can induce ICT in the sensor molecule upon coordinating with Hg^{2+} . The constructed sensor (BTABN) is therefore expected to meet the designed demand.

BTABN was tried to be synthesized by two routes. One is a four-step reaction process, as shown in Scheme 1. Intermediate 2, 3 and BTABN can be easily purified by column chromatography, and BTABN can be obtained successfully with 53.2% yield. In the other method, 3,9-dithia-6-monoazaundecane (DMA) is first prepared by bis(2-chloroethyl)amine hydrochloride and EtSH according to Ref. [28], then, reacted with *N*-*n*-butyl-4-bromo-1,8-naphthalimide.

The second method is one step less than the first method, but the reaction system is complicated and the purification of the target product is difficult, which may be result from the instability of DMA.

Sensitivity of BTABN to pH

In order to examine the disturbance of proton to the detection of Hg^{2+} , the UV–vis absorption and fluorescence spectra of BTABN in EtOH/Britton–Robinson buffer (1/2, v/v) solutions with different pH values were determined (Figs. 1 and 2). The spectra did not show obvious change from pH 2.11 to 10.93, which well matches the above design idea. This pH insensitivity of BTABN is beneficial to the detection of Hg^{2+} in different media.

Sensing behaviors of BTABN to Hg^{2+}

The response of UV–vis absorption spectra to Hg^{2+}

The response of BTABN to different metal ions, such as Na^+ , K^+ , Mg^{2+} , Ca^{2+} , Cr^{3+} , Mn^{2+} , Fe^{3+} , Fe^{2+} , Co^{2+} , Ni^{2+} , Cu^{2+} , Zn^{2+} , Cd^{2+} , Hg^{2+} and Pb^{2+} were investigated first by UV–vis absorption spectra. The EtOH/ H_2O (1/2, v/v) solution of BTABN (10 μM) is bright yellow in color without cations. Its absorption wavelength maximum was 436 nm and the molar extinction coefficient was $13,600 \text{ M}^{-1} \text{ cm}^{-1}$. Upon addition of the above cations (100 μM), the maximal weakening and broadening (toward short wavelength) of the

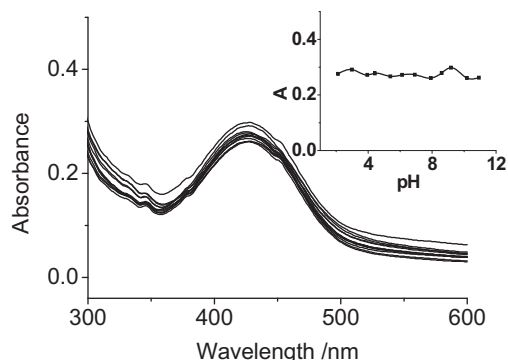


Fig. 1. UV–vis absorption response of BTABN upon different pH values. Solvent: EtOH/Britton–Robinson buffer (1/2, v/v); c: 10 μM . From top to bottom, pH: 9.18, 2.98, 8.60, 4.42, 2.11, 6.92, 6.12, 3.94, 5.38, 10.93, 10.18 and 7.92. Inset: plots of maximal absorbance (A) depending on the pH values.

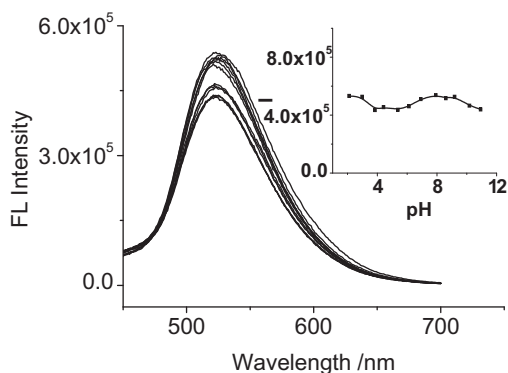


Fig. 2. Fluorescence response of BTABN upon different pH values. Solvent: EtOH/Britton–Robinson buffer (1/2, v/v); c: 10 μM ; λ_{ex} : 430 nm; slit width: 5 nm. From top to bottom, pH: 7.92, 2.11, 2.98, 9.18, 8.60, 6.92, 10.16, 6.12, 4.42, 10.93, 5.42 and 3.94. Inset: plots of fluorescence intensity maxima (I) depending on the pH values.

absorption peak at 436 nm were observed for Hg^{2+} among all the cations (Fig. 3).

When the concentrations of Hg^{2+} increase from 0 to 500 μM , the UV–vis absorption peak centered at 436 nm gradually reduced and disappeared along with a concomitant new peak centered at 376 nm appeared and gradually grew, and a 60 nm blueshift led to the solution changing from bright yellow to colorless, as shown in Fig. 4. The results suggest that BTABN has high selectivity to Hg^{2+} and can be used as a colorimetric and macroscopic sensor for Hg^{2+} in EtOH/ H_2O (1/2, v/v). A clear observed isosbestic point at 400 nm indicates the formation of BTABN/ Hg^{2+} complex [29].

Furthermore, the addition of Na^+ , K^+ , Mg^{2+} , Ca^{2+} , Cr^{3+} , Mn^{2+} , Fe^{3+} , Fe^{2+} , Co^{2+} , Ni^{2+} , Cu^{2+} , Zn^{2+} , Cd^{2+} , Pb^{2+} (100 μM) did not show significant effect on the UV–vis spectrum of the EtOH/ H_2O (1/2, v/v) solution of BTABN (10 μM) and Hg^{2+} (100 μM), as presented in Fig. 5. This result indicates that the system BTABN/ Hg^{2+} is hardly affected by these coexistent cations. According to the above data, BTABN is a reliable highly selective colorimetric sensor for Hg^{2+} in EtOH/ H_2O (1/2, v/v).

The response of fluorescence spectra to Hg^{2+}

To exam the sensing behavior of BTABN to Hg^{2+} in EtOH/ H_2O (1/2, v/v) further, the response of fluorescence spectra to various metal ions was investigated. The BTABN solution (10 μM) in the absence of Hg^{2+} emitted very weak fluorescence and the maximal fluorescence wavelength was 530 nm with the fluorescence quantum yield 0.101. Upon addition of Na^+ , K^+ , Mg^{2+} , Ca^{2+} , Cr^{3+} , Mn^{2+} , Fe^{3+} , Fe^{2+} , Co^{2+} , Ni^{2+} , Cu^{2+} , Zn^{2+} , Cd^{2+} , Hg^{2+} , Pb^{2+} (100 μM) to the solution of BTABN (10 μM), only Hg^{2+} caused a marked fluorescence enhancement with a fluorescence quantum yield 0.384 and a 14 nm blueshift, as shown in Fig. 6, and the response time was less than 1 min (Fig. 7). Fe^{3+} also aroused some fluorescence enhancement, but the fluorescence spectra did not show obvious blueshift or redshift. Accordingly, BTABN has high selectivity to Hg^{2+} and can be used as a “turn-on” fluorescent sensor for Hg^{2+} in EtOH/ H_2O (1/2, v/v).

Furthermore, it was found that the fluorescence of BTABN was gradually enhanced with the addition of Hg^{2+} from 0 μM to 500 μM (Fig. 8). The maximal fluorescence intensity (I) and the concentration of Hg^{2+} ($[\text{Hg}^{2+}]$) showed good linear relationship between Hg^{2+} concentration 10 μM and 100 μM ($[\text{Hg}^{2+}]/[\text{BTABN}]$) from 1 to 10 in the insets in Fig. 8, based on which the detection limit of BTABN was $1.27 \times 10^{-6} \text{ M}$, and the association constant was $1.12 \times 10^4 \text{ M}^{-1}$.

In order to determine the influence of other cations on the fluorescence detection of Hg^{2+} in EtOH/ H_2O (1/2, v/v), Na^+ , K^+ , Mg^{2+} , Ca^{2+} , Cr^{3+} , Mn^{2+} , Fe^{3+} , Fe^{2+} , Co^{2+} , Ni^{2+} , Cu^{2+} , Zn^{2+} , Cd^{2+} , Pb^{2+}

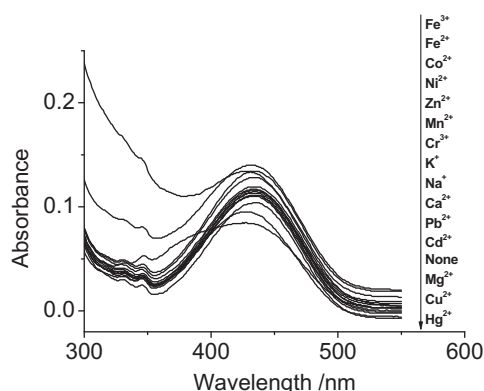


Fig. 3. UV–vis absorption spectra of BTABN with different metal ions. Solvent: EtOH/ H_2O (1/2, v/v); c: 10 μM .

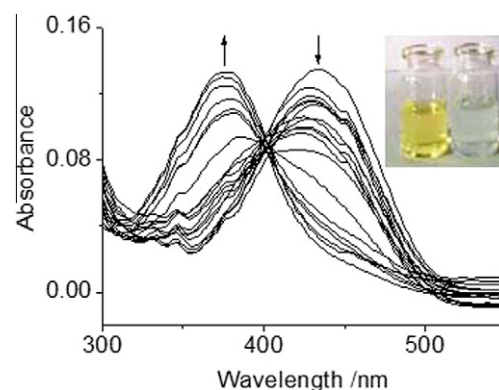


Fig. 4. UV–vis absorption spectra of BTABN with various concentrations of Hg^{2+} . Solvent: EtOH/ H_2O (1/2, v/v); c: 10 μM . From top to bottom at 436 nm, the equiv. of Hg^{2+} : 0, 0.3, 0.5, 0.7, 1, 3, 5, 7, 8, 9, 10, 12, 14, 16, 18, 20, 30 and 50. Inset: color of the solutions before (yellow) and after (colorless) addition of Hg^{2+} . (For interpretation of the references to color in this figure legend, the reader is referred to the web version of this article.)

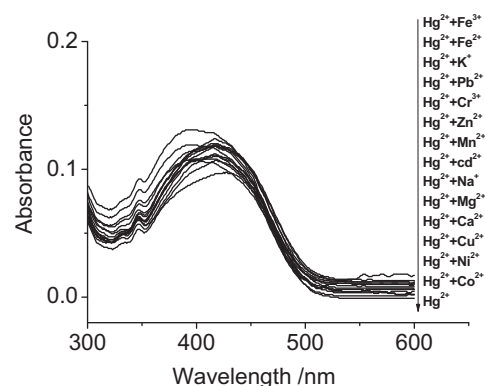


Fig. 5. Effects of coexisting ions on the UV–vis absorption spectra of BTABN and Hg^{2+} . Solvent: EtOH/ H_2O (1/2, v/v); c: 10 μM for BTABN and 100 μM for metal ions.

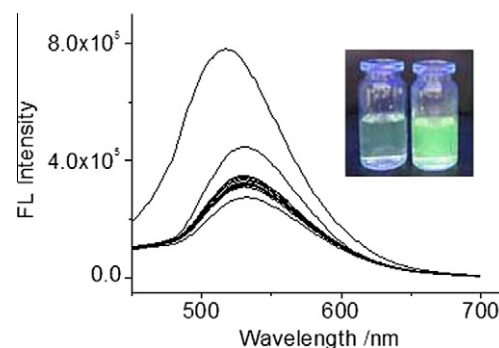


Fig. 6. Fluorescent spectra of BTABN with different metal ions. Solvent: EtOH/ H_2O (1/2, v/v); c: 10 μM for BTABN and 100 μM for metal ions; λ_{ex} : 436 nm; slit width: 5 nm. From top to bottom: Hg^{2+} , Fe^{3+} , Zn^{2+} , Cr^{3+} , Co^{2+} , Cu^{2+} , none, Ca^{2+} , Cd^{2+} , Ni^{2+} , Mg^{2+} , Fe^{2+} , Pb^{2+} , K^+ , Mn^{2+} , Na^+ . Inset: fluorescence of the solutions before (very weak) and after (green) addition of Hg^{2+} . (For interpretation of the references to color in this figure legend, the reader is referred to the web version of this article.)

(100 μM) were added to the solution of BTABN (10 μM) and Hg^{2+} (100 μM). All the cations showed negligible disturbance except for Fe^{3+} quenching the fluorescence slightly (Fig. 9).

Binding stoichiometry and sensing mechanism

To explore the possible binding mode of Hg^{2+} and BTABN, Job's plot analysis was carried out. The difference of the absorbance

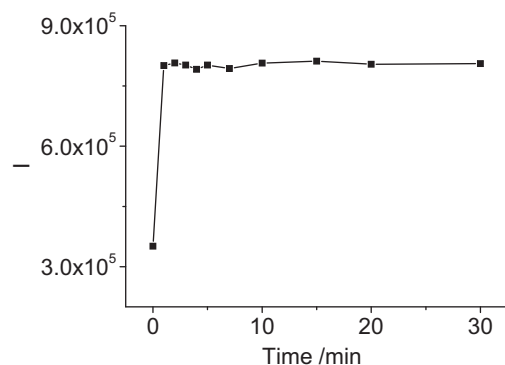


Fig. 7. Time response of BTABN to Hg^{2+} . Solvent: EtOH/ H_2O (1:2, v/v); c: 10 μM for BTABN and 100 μM for Hg^{2+} ; λ_{ex} : 436 nm; slit width: 5 nm.

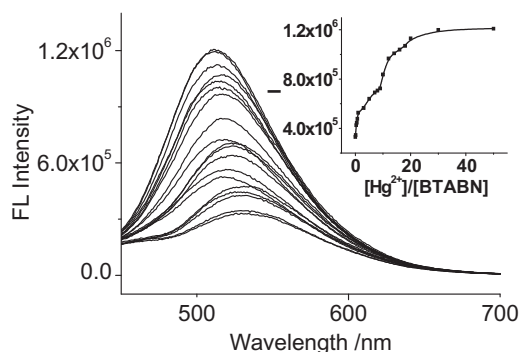


Fig. 8. Fluorescence spectra of BTABN with various concentrations of Hg^{2+} . Solvent: EtOH/ H_2O (1/2, v/v); c: 10 μM for BTABN and 0–500 μM for Hg^{2+} ; λ_{ex} : 436 nm; slit width: 5 nm. From bottom to top, the equiv. of Hg^{2+} : 0, 0.1, 0.3, 0.5, 0.7, 1, 3, 5, 7, 8, 9, 10, 12, 14, 16, 18, 20, 30, and 50. Inset: the relationship between the maximal fluorescence intensity (I) and the concentration of Hg^{2+} .

before (A_0) and after (A) addition of Hg^{2+} at 436 nm exhibited a maximum when $[\text{Hg}^{2+}]/[\text{BTABN} + \text{Hg}^{2+}]$ was 0.5 (Fig. 10), which indicates the 1:1 stoichiometry between Hg^{2+} and BTABN.

To further seek the detailed information on the complex of Hg^{2+} and BTABN, ^1H NMR spectra of BTABN before and after addition of Hg^{2+} were tested (Fig. 11). As the results of addition of Hg^{2+} , the signals of the protons in the CH_2 linked to the S atom remarkably shifted downfield 0.64 (3.32–2.68) ppm (c), and 0.54 (2.99–2.45) ppm (b), respectively, the peak of the proton (a) in the terminal CH_3 in SCH_2CH_3 moved from 1.17 to 1.30 ppm, and the

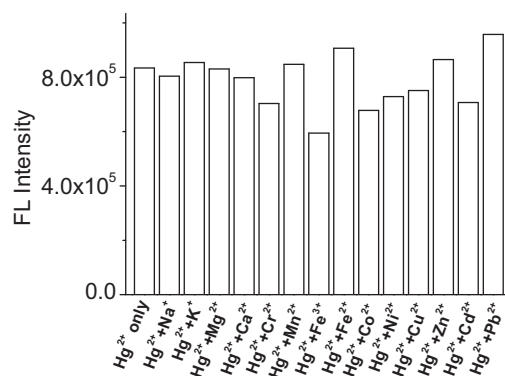


Fig. 9. Effects of coexist ions on the fluorescence maxima of BTABN and Hg^{2+} . Solvent: EtOH/ H_2O (1/2, v/v); c: 10 μM for BTABN and 100 μM for metal ions; λ_{ex} : 436 nm; slit width: 5 nm.

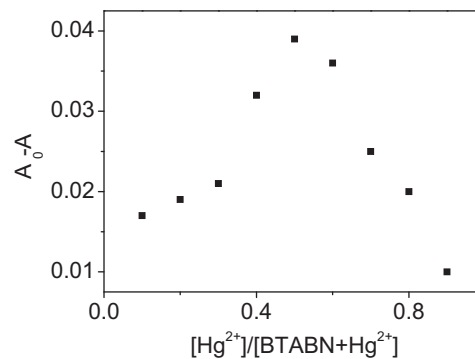


Fig. 10. Job's plot for Hg^{2+} versus BTABN. Solvent: EtOH/ H_2O (1/2, v/v); total concentration ($[\text{BTABN} + \text{Hg}^{2+}]$): 50 μM ; A_0 and A : Absorbance before and after addition of Hg^{2+} at 436 nm, respectively.

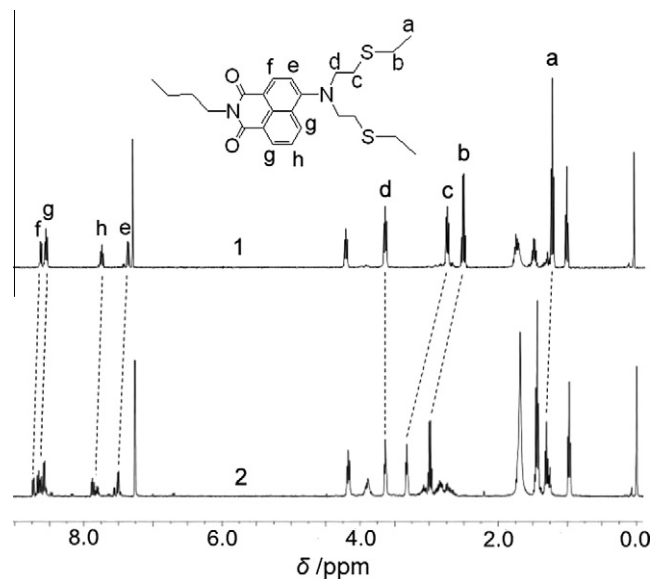
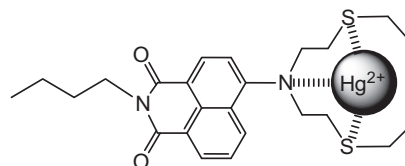


Fig. 11. ^1H NMR spectra of BTABN before (1) and after (2) addition of Hg^{2+} .



Scheme 2. Proposed complexation mechanism of BTABN with Hg^{2+} .

peak corresponding to the proton (d) in the CH_2 attached to the N atom in C-4 position of BTABN moved from 3.58 to 3.63 ppm. In addition, the peaks of the aryl protons neighboring to the N atom (e, f and h) shifted from 7.31, 8.62 and 7.68 to 7.51, 8.73 and 7.88 ppm respectively, and the peak of the aryl protons (g) splitted and shifted from 8.49 to 8.58 and 8.66 ppm. These data indicate that the S and N atoms participate in the coordination of BTABN and Hg^{2+} and BTABN binds Hg^{2+} via a tridentate chelation. Consequently, the proposed complex mechanism of BTABN with Hg^{2+} is given as Scheme 2.

Conclusions

In summary, new fast responsive colorimetric and “turn on” fluorescent Hg^{2+} sensor 4-(bis(2-(ethylthio)ethyl)amino)-N-n-butyl-1,8-naphthalimide (BTABN) was successively designed and

synthesized. BTABN was almost not sensitive to proton in a wide range of pH, but highly selective and sensitive to Hg^{2+} in EtOH/ H_2O (1/2, v/v). The detection can be carried out in aqueous solutions and a large number of biologically relevant ions show no significant interferences. BTABN binds Hg^{2+} via a tridentate chelation to the S and N atoms, which results in a 1:1 complex. The joint contribution of the PET and ICT process can achieve highly selective and sensitive colorimetric and “turn-on” fluorescent detection of metal ions.

Acknowledgments

The project supported by the National Natural Science Foundation of China (21074085), the open research foundation of the National Engineering Laboratory for Modern Silk, Soochow University (SS115801) and the Priority Academic Program Development of Jiangsu Higher Education Institutions.

Appendix A. Supplementary material

Supplementary data associated with this article can be found, in the online version, at <http://dx.doi.org/10.1016/j.saa.2012.11.113>.

References

- [1] P.B. Tchounwou, W.K. Ayensu, N. Ninashvili, D. Sutton, *Environ. Toxicol.* 18 (2003) 149–175.
- [2] D.W. Boening, *Chemosphere* 40 (2003) 1335–1351.
- [3] J.H. Hwa, J.H. Lee, S. Shinkai, *Chem. Soc.* 40 (2011) 4464–4474.
- [4] K. Kaur, R. Saini, A. Kumar, V. Luxami, N. Kaur, P. Singh, S. Kumar, *Coord. Chem. Rev.* 256 (2012) 1992–2028.
- [5] H.-F. Shi, Q. Zhao, Z.-F. An, W.-J. Xu, S.-J. Liu, W. Huang, *Prog. Chem.* 22 (2010) 1741–1752.
- [6] E.M. Nolan, S.J. Lippard, *Chem. Rev.* 108 (2008) 3443–3480.
- [7] S.-H. Yoon, A.E. Albers, A.-P. Wong, C.-J. Chang, *J. Am. Chem. Soc.* 127 (2005) 16030–16031.
- [8] S. Sumiya, T. Sugii, Y. Shiraishi, T. Hirai, *J. Photochem. Photobiol. A* 219 (2011) 154–158.
- [9] S. Guha, S. Lohar, I. Hauli, S.K. Mukhopadhyay, *Talanta* 85 (2011) 1658–1664.
- [10] H.-G. Wang, Y.-P. Li, S.-F. Xu, Y.-C. Li, C. Zhou, X.-L. Fei, L. Sun, C.-Q. Zhang, Y.-X. Li, Q.-B. Yang, X.-Y. Xu, *Org. Biomol. Chem.* 9 (2011) 2850–2855.
- [11] H.N. Kim, S.W. Nam, K.M.K. Swamy, Y. Jin, X.-Q. Chen, Y. Kim, S. Kim, S. Park, J.-Y. Yoon, *Analyst* 136 (2011) 1339–1343.
- [12] M.-L. Liu, W.-T. Yin, Z. Yang, J.-L. Li, Z. Shi, *Chinese J. Org. Chem.* 31 (2011) 39–53.
- [13] Y.-J. Gong, X.-B. Zhang, Z. Chen, Y. Yuan, Z. Jin, L. Mie, J. Zhang, W.-H. Tan, G.-L. Shen, R.-Q. Yu, *Analyst* 137 (2012) 932–938.
- [14] W.-J. Huang, W.-H. Wu, J.-X. Liang, *Acta Chim. Sin.* 70 (2012) 873–880.
- [15] W. Liu, J. Chen, L. Xu, J. Wu, H. Xu, H. Zhang, P. Wang, *Spectrochim. Acta A* 85 (2012) 38–42.
- [16] B. Tang, L. Cui, K. Xu, L. Tong, G. Yang, L. An, *Chem Biochem.* 9 (2008) 1159–1164.
- [17] M. Zhu, M.-J. Yuan, X.-F. Liu, J.-L. Xu, J. Lv, C.-S. Huang, H.-B. Liu, Y.-L. Li, S. Wang, D.-B. Zhu, *Org. Lett.* 10 (2008) 1481–1484.
- [18] H. Zheng, X.-J. Zhang, X. Cai, Q.-N. Bian, M. Yan, G.-H. Wu, X.-W. Lai, Y.-B. Jiang, *Org. Lett.* 14 (2012) 1986–1989.
- [19] T. Chen, W.-P. Zhu, Y.-F. Xu, S.-Y. Zhang, X.-J. Zhang, X.-H. Qian, *Dalton Trans.* 39 (2010) 1316–1320.
- [20] C. Hou, A.M. Urbanec, H.-S. Cao, *Tetrahedron Lett.* 52 (2011) 4903–4905.
- [21] J. Jiang, W. Liu, J. Cheng, L.-Z. Yang, H. Jiang, D.-C. Bai, W.-S. Liu, *Chem. Commun.* 48 (2012) 8371–8373.
- [22] J.-X. Wang, C.-G. Bi, B. Yuan, Z.-S. Li, W.-H. Qiao, J.-M. Luan, *Petrochem. Technol.* 35 (2006) 464–468.
- [23] X.-F. Guo, B.-C. Zhu, Y.-Y. Liu, Y. Zhang, L.-H. Jia, X.-H. Qian, *Chinese J. Org. Chem.* 26 (2006) 504–507.
- [24] J.E. Elbert, S. Paulsen, L. Robinson, S. Elzey, K. Klein, *J. Photochem. Photobiol. A* 169 (2005) 9–19.
- [25] D. Staneva, I. Grabchev, J.P. Soumillion, V. Bojinov, *J. Photochem. Photobiol. A* 189 (2007) 192–197.
- [26] V.B. Bojinov, I.P. Panova, *Dyes Pigments* 80 (2009) 61–66.
- [27] M.-K. Yan, C. Zheng, J. Yin, Z.-F. An, R.-F. Chen, X.-M. Feng, J. Song, Q.-L. Fan, W. Huang, *Syn.Met.* 162 (2012) 641–649.
- [28] M. Tanaka, M. Nakamura, T. Ikeda, K. Ikeda, H. Ando, Y. Shibutani, S. Yajima, K. Kimura, *J. Org. Chem.* 66 (2001) 7008–7012.
- [29] B. Valeur, J. Pouget, J. Bouson, M. Kaschke, N.P. Ernsting, *J. Phys. Chem.* 96 (1992) 6545–6549.